



LAWRENCE
LIVERMORE
NATIONAL
LABORATORY

CO₂-Rock Interactions in EGS-CO₂: New Zealand TVZ Geothermal Systems as a Natural Analog

T. J. Wolery, S. A. Carroll

May 20, 2010

GRC Annual Meeting
Sacramento, CA, United States
October 24, 2010 through October 27, 2010

Disclaimer

This document was prepared as an account of work sponsored by an agency of the United States government. Neither the United States government nor Lawrence Livermore National Security, LLC, nor any of their employees makes any warranty, expressed or implied, or assumes any legal liability or responsibility for the accuracy, completeness, or usefulness of any information, apparatus, product, or process disclosed, or represents that its use would not infringe privately owned rights. Reference herein to any specific commercial product, process, or service by trade name, trademark, manufacturer, or otherwise does not necessarily constitute or imply its endorsement, recommendation, or favoring by the United States government or Lawrence Livermore National Security, LLC. The views and opinions of authors expressed herein do not necessarily state or reflect those of the United States government or Lawrence Livermore National Security, LLC, and shall not be used for advertising or product endorsement purposes.

CO₂-Rock Interactions in EGS-CO₂: New Zealand TVZ Geothermal Systems as a Natural Analog

Thomas J. Wolery and Susan A. Carroll

Lawrence Livermore National Laboratory
Livermore, California 94551

Key words: geochemistry, modeling, Taupo Volcanic Zone, Broadlands-Ohaaki, EGS, CO₂

Abstract

High levels of CO₂ are found in the Broadlands-Ohaaki geothermal system in the Taupo Volcanic Zone of New Zealand. The system has been studied for over forty years, and over that time a significant body of information on rock-water-gas interaction in the system has been obtained. CO₂-rich water flows up from fractures in the low permeability basement greywacke into the overlying reservoir, which is dominated by rhyolites, dacite, pyroclastics, and some lake sediment. It is an excellent natural analog for rock-water-gas interactions that would occur in an EGS system using CO₂ as a heat extraction fluid. In terms of rock chemistry and mineralogy, this is a more “felsic” system (e.g., rhyolite, granite) that might be expected to yield less reaction with CO₂ than a more “mafic” system (e.g., basalt, gabbro). Nevertheless, a significant amount of reaction does occur. We are conducting new geochemical modeling studies, laboratory experiments, and a field experiment to develop an improved understanding of the water-rock-gas interactions in this system as it relates to being a natural analog of an EGS-CO₂ system. Here we review the most pertinent known aspects of what is known about the Broadlands-Ohaaki system and describe initial geochemical modeling studies of the deep fluid in the natural system using more recent and extensive thermodynamic data

than used in earlier, published studies. Attention is focused on the role of sheet silicates (micas, chlorites, and clays) in stable mineral assemblages.

Introduction

EGS-CO₂ refers to Enhanced Geothermal Systems in which supercritical CO₂ is supplied as the heat transmission fluid replacing water (Brown, 2000). This is a useful concept where there are reservoirs of hot rock lacking much native water. It would also provide some geologic sequestration of CO₂. Pruess (2006) used numerical simulations to evaluate CO₂ as a heat transmission fluid. He concluded that it was superior to water in this role, but that major uncertainties remained regarding fluid-rock interactions. There has been much recent interest in fluid-rock interactions in the context of both EGS-CO₂ (maximum temperatures of 250°C or higher) and more “conventional” underground carbon sequestration (maximum temperatures generally < 120°C). Fluid-rock interactions in both contexts will depend on such factors as temperature, pressure, abundance of CO₂ and other acid gases (e.g., H₂S and SO₂), H₂O abundance, fluid phase compositions, host rock type, and physical properties of the rock, including porosity and permeability. Common issues of concern include changes in porosity and permeability, and trapping of

CO₂ by dissolution in water and precipitation in carbonate minerals.

Xu et al. (2008) conducted numerical studies of fluid-rock interactions pertinent to EGS-CO₂. They considered a general model for a fully developed system comprised of three zones: an inner zone (1) in which supercritical CO₂ has displaced all aqueous phase, an intermediate zone (2) in which supercritical CO₂ coexists with a CO₂-saturated aqueous phase, and an outer zone (3) in which an aqueous phase containing dissolved CO₂ is present. Xu et al. focused on rock-fluid interactions mediated by the aqueous phase in zones 2 and 3. They did not model a particular site, but did utilize mineralogical data from the European Hot Dry Rock research site at Soultz-sous-Forêts in northern France. The reservoir there is composed of granite with alteration products of clay and carbonate. The modeled system was one-dimensional and apparently isothermal at 200°C. Ambient water equilibrated with a CO₂ partial pressure of 350 bar (resulting in a dissolved CO₂ concentration of 1.07 molal) was flowed into the system, displacing normal ambient water. The low pH of the high CO₂-water resulted in dissolution of primary calcite, K-feldspar, and chlorite, and precipitation of clays and secondary carbonates. Porosity significantly decreased near the inlet boundary.

The reactivity of supercritical CO₂ with minerals in zone 1 is not well established. Xu et al. (2008) considered that the dry fluid might be largely unreactive owing to the nonpolar nature of the CO₂ molecule, but that porosity-permeability might be increased somewhat by removal of water of hydration from some minerals. McGrail et al. (2009) have questioned this view in the context of lower-temperature CO₂ sequestration, noting that displacing all

aqueous solution from the rock may be difficult and pointing out that some H₂O may be dissolved in the supercritical CO₂ phase (H₂O may be chemically reactive in such a phase). Furthermore, Regnault et al. (2005) reported experiments at 200°C in which minerals appreciably reacted with supercritical CO₂ in “water-free” systems (but we note these systems may not have been chemically free of H₂O).

In general, CO₂ and other fluid components are expected to react less strongly with rocks of a more felsic nature (e.g., granites, many sandstones) than rocks of a more mafic nature (e.g., andesite, basalt, peridotite), owing to the less reactive nature (thermodynamic, kinetic) of the dominant minerals. A considerable amount of chemical reaction could occur even in the more felsic systems, driven by fluid flow, temperature gradients, fluid mixing, and boiling.

We are conducting a research program on fluid-rock interactions pertinent to EGS-CO₂. We are first drawing on relevant information from natural analog systems, which include the geothermal systems of the Taupo Volcanic Zone (TVZ) in New Zealand. The information obtained (insights, concepts, data, and models) will be used to design laboratory experiments and a future field experiment. Geochemical reaction-path and reactive transport calculations will be used to provide a framework for modeling the relevant fluid-rock interactions in natural geothermal systems and EGS-CO₂ systems. The New Zealand TVZ geothermal systems offer insight into CO₂-rich fluid interactions with felsic rocks (greywackes, rhyolites, and ignimbrites) at EGS-CO₂ relevant temperatures (e.g., up to 300-400°C).

The Broadlands-Ohaaki Geothermal System

The Broadlands-Ohaaki field is a CO₂-rich system in the TVZ. Lee and Bacon (2000) give an operational history of the field. Exploitation began with the opening of the power station in 1989, following scientific and engineering studies going to the 1960s. The field has been impacted by changes going back to the 1968-1971 period. In 1993, the station energy production began declining and compensatory measures began. Colder, shallower water was observed entering the reservoir, and pressures and temperatures dropped. Boiling conditions remained in most of the production zone. Temperatures held in the deepest wells. In recent years, part of the system has rebounded somewhat (Mroczek, 2010, private communication).

Geologically, the reservoir consists of rhyolites, dacite, ignimbrites, and related pyroclastics and reworked material, plus some lacustrine sediment (cf. Hedenquist, 1990; Lee and Bacon, 2000). The reservoir rests on a basement of faulted greywacke (Torlesse Formation), which is thought to be largely impermeable except for fractures related to the faults. The basement depth varies between about 1000m and 2500m, and the temperature at the top of the basement is about 300±25°C (Hedenquist, 1990, Figure 3).

The literature on the geology and geochemistry of the Ohaaki geothermal system and related systems in the TVZ is extensive. Some notable papers summarizing information and previous literature pertaining to the geochemistry of Ohaaki include Browne and Ellis (1970), Giggenbach (1989), Hedenquist (1990), Lonker et al. (1990), Simmons and Browne (2000), and Christenson et al. (2002).

Hedenquist (1990) provides a detailed summary of the system in its earlier, less altered state. The fluid chemistry is affected by mixing of shallower dilute water with “chloride-rich” (in fact only the equivalent of ~ 0.05m NaCl) high-CO₂ deep water, which rises from the basement. Pressures and temperatures in the deeper and interior parts of the reservoir tend to approximate boiling conditions. The principal hydrothermal mineral assemblage at 260°C (600-800m depth) is quartz-albite-illite-adularia-calcite-chlorite-pyrite. Adularia is simply secondary K-feldspar. “Illite” may refer to illite or K-mica (muscovite). Quartz and calcite are common and abundant. Calcite is known to form due to boiling ($2\text{HCO}_3^- + \text{Ca}^{2+} = \text{CaCO}_3\downarrow + \text{CO}_2\uparrow + \text{H}_2\text{O}$). In the cooler, marginal parts of the system, alteration minerals include kaolinite, Ca-montmorillonite, illite-smectite, siderite, leucoxene, and mordenite. The high temperature assemblage is quoted to be stable to about 305°C, based on a study by Browne and Ellis (1970), relying in turn on thermodynamic data and stability diagrams taken from Hemley and Jones (1964). Following others (e.g., Browne, 1978), Hedenquist notes that the sheet silicates are semi-quantitative indicators of temperature and fluid composition. Montmorillonite forms mainly below about 140°C, illite is usually restricted to temperatures above 230°C, and interstratified illite-smectite forms at intermediate temperatures. Kaolinite occurs where acid conditions have developed due to sulfide oxidation.

Analyses of water samples typically reflect degassing (low CO₂, moderate to elevated pH; cf. Hedenquist, 1990, Table 3). The CO₂ content of the deep fluid is inferred from multiple lines of evidence. The most direct comes from analysis of HCO₃ in downhole samples that were collected into caustic

(NaOH), thus chemically trapping the CO₂ (cf. Hedenquist, 1990, Table 5). One is the high CO₂ content of recovered gas samples (cf. Hedenquist, 1990, Table 4). A problem is that gas samples might or might not be coeval with water samples. One approach has been to use the excess enthalpy of total discharge to estimate the reservoir steam fraction and to use that as a basis for reconstructing the in situ fluid. Another has been to assume in situ vapor-liquid equilibrium. Yet another approach is to use boiling curve deviation for deep water samples to estimate CO₂ content. Using this approach, Hedenquist (1990) estimates 2.7 wt% CO₂ or 0.6 mol/kg for well BR15. He prefers the BR15 composition as best approximating the parent fluid composition based on its position on an enthalpy-chloride mixing diagram (his Figure 8). This is one of the deeper wells (1067m at the time). He also estimates a corresponding H₂S content of 0.015 wt% or 0.0044 mol/kg. We note that estimates of the CO₂ content of the deep fluid vary. The water samples collected in caustic and reported by Hedenquist (1990, Table 5) range from 0.02 -0.48 mol/kg CO₂. A value “from caustic” is not available for BR15.

Christenson et al. (2002) provided an updated analysis of the Ohaaki reservoir chemistry including data from the 1997-1999 time period (when the field was altered to a greater extent by exploitation). They give a more extensive analysis of fluid mixing, using additional chemical and isotopic data. Interestingly, they also present the results of some reaction path calculations of the reaction of inferred magmatic gas condensates with the basement greywacke, illustrating the role of sulfur species in controlling redox and pH. We note that Christenson et al. (Table 3) present analyses of gas samples from the Ohaaki field that include examples that are more CO₂-rich

than those in an earlier data set presented by Hedenquist (1990, Table 4). This would seem to imply that deep parent waters might contain higher concentrations of dissolved CO₂ than would be inferred from the earlier gas phase data.

Simmons and Browne (2000) addressed hydrothermal minerals and precious metals in the Ohaaki-Broadlands system. As part of their study, they used the codes SOLVEQ and CHILLER (e.g., Reed, 1982; Reed and Spycher, 1985) to construct a model of the deep parent water and then model the effects of boiling and mixing in the geothermal reservoir. The parent water was based on an analysis of BR25 water as reported by Hedenquist (1990). This was equilibrated with quartz, pyrite, chalcopyrite, albite, muscovite, and two chlorites, clinocllore and daphnite. The equilibrated water was found to be slightly undersaturated with calcite and K-feldspar. Such an equilibration process is in part necessary because the chemical analysis of the well water does not include data for some dissolved components, such as aluminum and copper. The BR25 analysis pertains to a degassed sample containing 300 mg/kg HCO₃ (about 0.005 molal). Hedenquist (1990, Table 5) does not include a “from caustic” result for BR25. Simmons and Browne do not discuss how they corrected for the degassing, and the input for the computer run to create the deep parent water is not included in their appendix. The appendix does include the inputs for the reaction path runs. These inputs suggest addition of about 0.28 mol/kg CO₂. H₂O (steam) may also have been added, as the chloride in the inputs seems low compared with the cited source. Small concentrations of gold, silver, zinc, and lead also appear in the water on these inputs, but it is not clear how these were originally specified (proxy concentration or assumption of additional mineral equilibria).

The Ohaaki geothermal system appears to be an excellent natural analog for zone 3 (and possibly zone 2) of an EGS-CO₂ system in similar (felsic) rocks (e.g., greywackes, rhyolites, equivalent pyroclastics). The most relevant part of the system is in the basement and deeper, inner parts of the reservoir. We note that the inferred CO₂ content of the deep parent water (0.6 mol/kg, with a plausible range of 0.3-0.9 mol/kg) is about half the 1.07 mol/kg used in the modeling study of Xu et al. (2008).

New Geochemical Calculations

We begin our study with new geochemical modeling calculations. We do this because we want to (a) compare modeling results with existing geochemical data and previous modeling and (b) to look for any new insights into Ohaaki geochemistry. For these calculations, we use EQ3/6 (e.g., Wolery and Jarek, 2003) and a thermodynamic database (Wolery and Jove-Colon, 2007) originally developed for use on the Yucca Mountain Project. A significant part of this database is based on SUPCRT92 (cf. Johnson et al., 1992, and sources cited therein). This part is likely consistent with the databases used in the previously cited modeling by Simmons and Browne (2000) and Christenson et al. (2002). However, we note two differences. First, for the database used here, the SUPCRT92 data were corrected for consistency with a revised standard Gibbs energy of formation for SiO_{2(aq)}, following the lead of Rimstidt (1997). This change implies that quartz is more soluble than implied by the older data. Second, this database includes new estimates of data for a wide variety of sheet silicates including various clays, using a slightly revised predictive methodology similar to that used earlier by Wolery (1978).

To model the deep parent water, we follow Hedenquist (1990) and base it on the BR15 well water analysis. The calculation takes 1 kg of the model water to 300°C adds Hedenquist's recommended 0.6 mole CO₂ and 0.0044 mole H₂S. This model is sufficient to describe the major features of the water chemistry, although as noted above, it is necessary to assume in addition certain mineral equilibria to obtain concentrations for trace components such as aluminum.

Figure 1 shows the effect on pH of adding the gases. Here the calculation is run out to 4 moles of CO₂ (and proportionate H₂S). Note that at 4 mol/kg CO₂, the pH is decreasing to about neutral (5.65 at 300°C), while at 0.6 mol/kg, the pH is definitely on the alkaline side. This result is not sensitive to whether or not minerals are allowed to precipitate. If they are, very minor carbonate is present over most of the range shown, and some quartz is present throughout. For comparison, Figure 1 shows the effect of adding the same gases to 0.05m NaCl solution (which has about the same ionic strength as the BR15 water). The pH curve for this case is substantially lower. In the case of the BR15 water, the presence of the initial 310 mg/kg HCO₃⁻ acts to oppose the formation of hydrogen ions (per the law of mass action) according to the reaction $\text{CO}_{2(\text{aq})} + \text{H}_2\text{O} = \text{H}^+ + \text{HCO}_3^-$.

Figure 2 shows the log K values (from the thermodynamic database cited above) as a function of temperature for the reactions $\text{CO}_{2(\text{aq})} + \text{H}_2\text{O} = \text{H}^+ + \text{HCO}_3^-$ and $\text{H}_2\text{O} = \text{H}^+ + \text{OH}^-$. As temperature increases, CO₂ becomes a weaker acid. Also, water dissociates less into hydrogen and hydroxide ions. Because $\text{pH}(\text{neutral}) = -\frac{1}{2} \log K$ for this reaction, the value of neutral pH becomes smaller (Figure 3). These factors

need to be kept in mind in comparing higher temperature EGS with generally lower temperature carbon sequestration scenarios.

The CO₂ content of the deep hot zone water is high but less than would be expected if supercritical CO₂ were present. Figure 4 shows the calculated CO₂ partial pressure associated with adding the gas. For comparison, the critical pressure of CO₂ is 73.8 bar (Span and Wagner, 1996). The partial pressure of pure water at 300°C is 85.8 bar (from the above cited thermodynamic database). Ambient total pressure at the top of the basement is presumably in the range 100-250 bars (normal hydrostatic), depending on location. It could be somewhat lower than normal hydrostatic due to the presence of boiling zones. To achieve saturation with a supercritical CO₂ phase, the CO₂ partial pressure would first have to match the total ambient pressure (to make the formation of a CO₂-dominated fluid phase possible). It would have to exceed the critical pressure of CO₂ for such a fluid to be considered supercritical. Lastly, this fluid couldn't have too much steam dissolved in it. The high partial pressures of H₂O at the top of the basement mean that any non-aqueous CO₂ here will be a guest component of subcritical steam.

To fully model the deep parent water, it is necessary to consider mineral equilibria. This is necessary for two reasons. First, the reported water analyses do not include certain trace components, such as aluminum and iron. Assuming that the water is saturated with minerals bearing such components is a reasonable means of completing the model. Second, it is desirable to determine if a given mineral assemblage is actually stable or not. There is a range of possible starting points here. Several deep well compositions are possible starting

points (we prefer BR15 as recommended by Hedenquist, 1990). There is also a range of potential mineral assemblages to consider.

Following Simmons and Browne (2000), we attempted to equilibrate BR15 water (which is very similar to the BR25 water they used) by reacting 0.6 moles each of pyrite (FeS₂), albite (NaAlSi₃O₈), muscovite (K-mica:

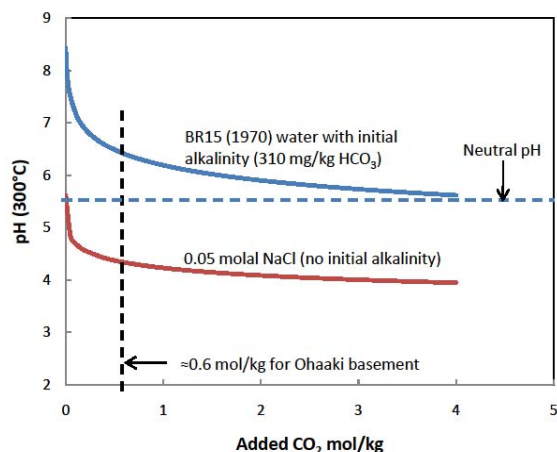


Figure 1. Effect on pH of adding CO₂ (and minor H₂S) to BR15 water (blue) and 0.05m NaCl (red) at 300°C.

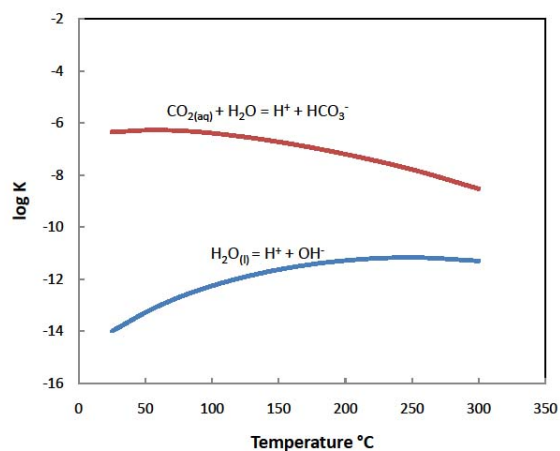


Figure 2. Equilibrium constants (log K) versus temperature for the reactions CO_{2(aq)} + H₂O = H⁺ + HCO₃⁻ (red) and H₂O = H⁺ + OH⁻ (blue).

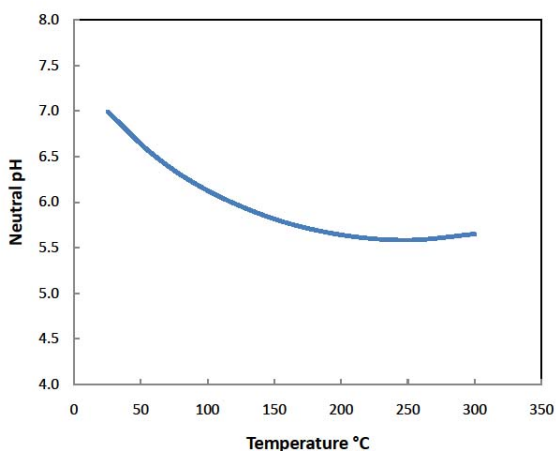


Figure 3. Neutral pH as a function of temperature.

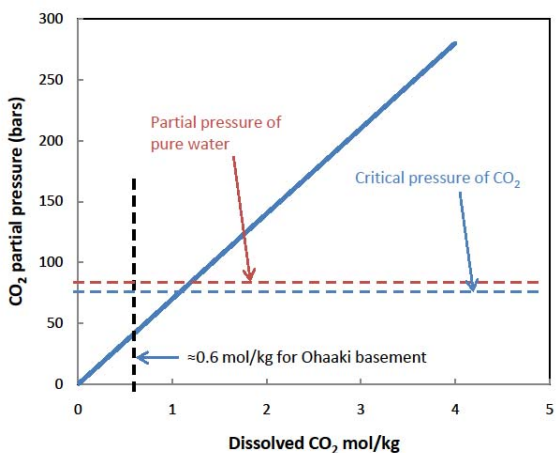


Figure 4. The increase in partial pressure of CO₂ resulting from the addition of gas to BR15 water at 300°C.

$\text{KAl}_3\text{Si}_3\text{O}_{10}(\text{OH})_2$), clinocllore (an Mg-chlorite: $\text{Mg}_5\text{Al}_2\text{Si}_3\text{O}_{10}(\text{OH})_8$), and daphnite (an Fe(II)-chlorite: $\text{Fe}_5\text{Al}_2\text{Si}_3\text{O}_{10}(\text{OH})_8$) and of 6 moles of quartz with 1 kg of water and 0.6 moles of CO₂ and 0.0044 moles of H₂S. These mineral mole numbers should be much more than sufficient to saturate the solution. We use a greater mole number for quartz for reasons that will be apparent below. Again following Simmons and Browne, we would then expect the resulting aqueous solution to be close to saturation

with K-feldspar (KAlSi_3O_8) and calcite (CaCO_3).

Figure 5 shows the results for the minerals. The blue columns represent the mole numbers of the mineral reactants at the start of the run. The red columns depict the mole numbers of the minerals present at the end of the run. It is apparent that the starting mineral assemblage is not stable. Almost all the quartz is consumed during the run. A higher amount of quartz was reacted than for other minerals in order to maintain the presence of some. This is reasonable, as quartz is highly abundant in the basement greywacke. The muscovite, clinocllore, and daphnite are gone. Five new minerals have appeared. There are significant amounts of ripidolite (a mixed Mg-Fe-chlorite: $\text{Mg}_3\text{Fe}_2\text{Al}_2\text{Si}_3\text{O}_{10}(\text{OH})_8$), montmorillonite (a common smectite: $(\text{Na},\text{K},\text{H},\text{Ca}_{0.5},\text{Mg}_{0.5})_{0.33}\text{Mg}_{0.33}\text{Al}_{1.67}\text{Si}_4\text{O}_{10}(\text{OH})_2$), and FeAl-celadonite (ferroaluminoceladonite: $\text{KFeAlSi}_4\text{O}_{10}(\text{OH})_2$). There are also very small amounts of nontronite (an Fe(III)-rich smectite: $(\text{Na},\text{K},\text{H},\text{Ca}_{0.5},\text{Mg}_{0.5})_{0.165}\text{Fe(III)}_2\text{Al}_{0.33}\text{Si}_{3.67}\text{O}_{10}(\text{OH})_2$) and minnesotaite (a sheet silicate similar to talc, with Fe replacing Mg: $\text{Fe}_3\text{Si}_4\text{O}_{10}(\text{OH})_2$). Ripidolite lies on the clinocllore-daphnite join. Therefore, most (but not all) of the “chlorite” in the system is retained. The FeAl-celadonite has some affinity to illite (represented in our thermodynamic database by the composition: $\text{K}_{0.6}\text{Mg}_{0.25}\text{Al}_{1.8}\text{Al}_{0.5}\text{Si}_{3.5}\text{O}_{10}(\text{OH})_2$), which is a mineral commonly reported in the higher temperature zone at Ohaaki. Celadonites generally occur as alteration products of basalts and intermediate volcanics. The presence of the montmorillonite is more unexpected, as smectite is generally not reported in the higher temperature zone, as is the disappearance of the muscovite.

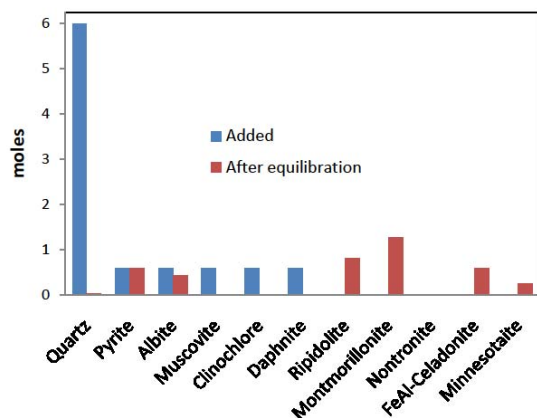


Figure 5. Equilibration of minerals from Simmons and Browne (2000) with BR15 water and 0.6 mol/kg CO₂ and 0.0044 mol/kg H₂S. Blue: minerals added. Red: minerals present after equilibration.

The pH at the end of this calculation is 6.49. This is slightly higher than the 6.41 that is obtained by reacting BR15 water with only the gases. The saturation index (SI = log Q/K, where Q is activity product and K is equilibrium constant) for calcite is -0.701, while that for K-feldspar is -0.436. The solution is somewhat more undersaturated with these minerals than would be expected.

Simmons and Browne (2000) did not note any changes to the mineral assemblage. This may have been because in their usage of SOLVEQ/CHILLER, they specified which minerals were allowed to form, and restricted this to the minerals they chose as reactants. We were substantially able to duplicate their calculation using an older database thought to better approximate the one they used, and disallowing the formation of non-reactant minerals. We used BR25 well water, adding gases in the proportion they apparently used.

Re-running the problem as we originally posed it, substituting 1.2 moles of ripidolite for 0.6 moles each of clinocllore and daphnite, we obtained results much as

expected. The change in the mineral assemblage is shown in Figure 6. Accounting for the change in treatment of “chlorite,” the results are much as expected. The muscovite is still eliminated and montmorillonite and Fe-Al celadonite still form in about the same proportions. However, much less quartz is destroyed. Also, a small amount of saponite (an Mg-rich smectite: (Na,K,H, Ca_{0.5},Mg_{0.5})_{0.33} Mg₃Al_{0.33}Si_{3.67}O₁₀(OH)₂) now forms instead of a small amount of minnesotaitite. We note that the chlorite mineral substitution has slightly shifted the overall chemistry of the system, because ripidolite is not at the 50:50 position on the clinocllore-daphnite joint, but rather closer to the clinocllore end (60:40). Thus, Mg replaces some Fe.

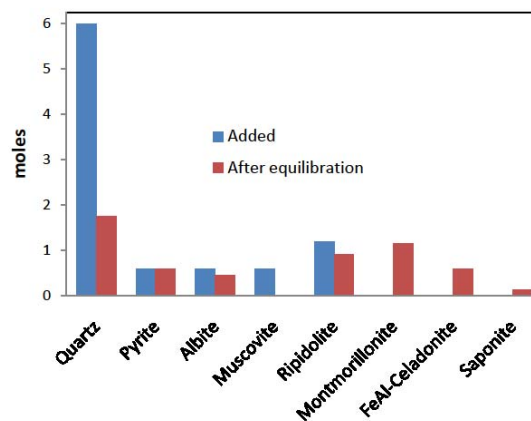


Figure 6. Equilibration of minerals, as in Figure 5, substituting ripidolite for clinocllore plus daphnite. Blue: minerals added. Red: minerals present after equilibration.

The pH is shifted to a slightly higher 6.55. K-feldspar is somewhat closer to saturation (SI = -0.180). However, calcite is more undersaturated (SI = -0.867).

Taking a different approach, we backed off on the number of reacted minerals and started with only quartz, pyrite, and albite. The result of this was that nearly negligible

amounts of the primary reactants were destroyed. Very small amounts of K-feldspar, calcite, and beidellite (an Al-rich smectite: $(\text{Na},\text{K},\text{H},\text{Ca}_{0.5},\text{Mg}_{0.5})_{0.33}\text{Al}_{2.33}\text{Si}_{3.67}\text{O}_{10}(\text{OH})_2$) formed. This implies that a run in which K-feldspar were also added would produce the same result, except that more K-feldspar would be present. The results of a run in which this was done is shown in Figure 7.

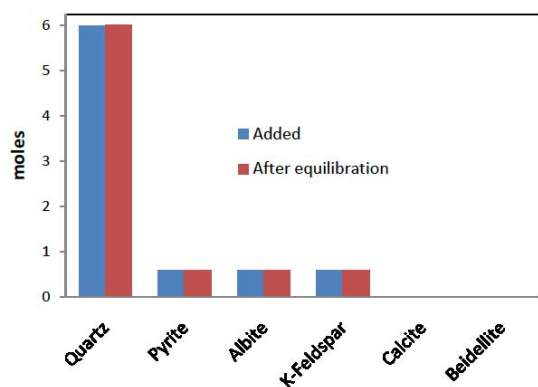


Figure 7. Equilibration of BR15 water plus added gas with quartz, pyrite, albite, and K-feldspar. Blue: minerals added. Red: minerals present after equilibration.

Because K-feldspar is one of the known important secondary minerals in the deep system at Ohaaki, we adopted the above system as a tentative base case and then examined the effect of adding one of a series of mica and chlorite minerals. In none of these cases was the reactant phase assemblage preserved. Only two of the cases (muscovite and ripidolite) will be described here. These exemplify the kinds of results obtained from the larger set. In the case of muscovite (Figure 8), the muscovite itself was destroyed. Some of the quartz and albite was consumed, the amount of K-feldspar increased, and a significant amount of beidellite was formed. The pH was 6.35, slightly lower than the values noted in the previous cases. Calcite was strongly

undersaturated ($\text{SI} = -1.718$). In the case of ripidolite (Figure 9), the ripidolite was partially consumed, along with some quartz and some albite. However, all of the K-feldspar is destroyed. Significant amounts of FeAl-celadonite, montmorillonite, and saponite are formed. The pH is again higher, about 6.54. K-feldspar, though destroyed, is not much undersaturated ($\text{SI} = -0.180$), and calcite is again more undersaturated ($\text{SI} = -0.867$).

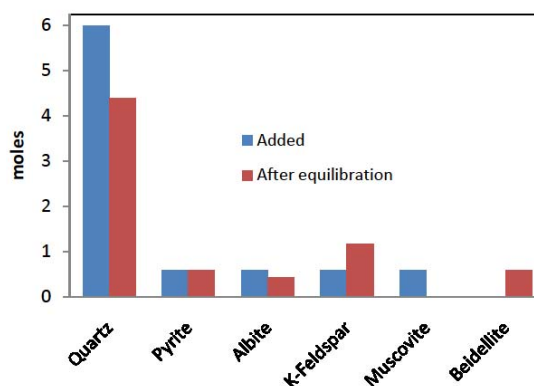


Figure 8. Equilibration of BR15 water plus added gas with quartz, pyrite, albite, K-feldspar, and muscovite. Blue: minerals added. Red: minerals present after equilibration.

These results raise some questions about the stability of reported secondary mineral assemblages. The problem involving the combination albite-K-feldspar-muscovite is not hard to explain, as on activity diagrams (cf. Simmons and Browne, 2000, Figure 11A) it is apparent that equilibrium among all three (in the presence of quartz) requires, at a given temperature, falling on a specific point where three stability fields meet. The muscovite field forms a wedge between the two feldspars extending up to the three-mineral equilibrium point. Apart from that point, one would expect to see at most only

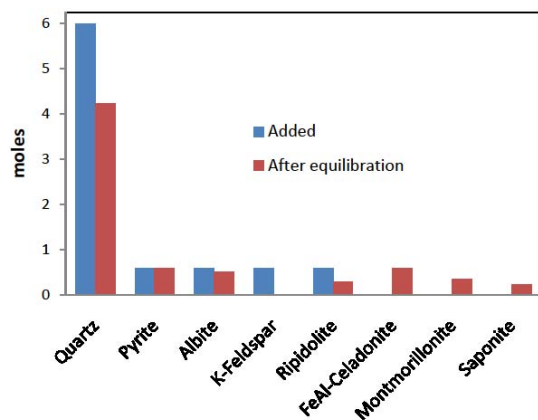


Figure 9. Equilibration of BR15 water plus added gas with quartz, pyrite, albite, K-feldspar, and ripidolite. Blue: minerals added. Red: minerals present after equilibration

two of these three minerals in a stable assemblage. The same applies if muscovite is replaced by illite of composition $K_{0.6}Mg_{0.25}Al_{1.8}Al_{0.5}Si_{3.5}O_{10}(OH)_2$. The problem regarding ripidolite (chlorite) and K-feldspar is more difficult to explain. The calculations suggest that they do not stably exist together at 300°C in the presence of other expected secondary phases.

Hedenquist (1990) made reference to the assemblage quartz-albite-illite-adularia-calcite-chlorite-pyrite as “the principal mineral assemblage” at 260°C. While the exact temperature could be a factor in thermodynamic stability, the larger point is that this assemblage is not necessarily stable at any specific temperature. It is more likely that it is a composite of smaller stable assemblages representing not only a range of temperature but also a range of local chemistries within a larger volume. Kinetically controlled disequilibrium might also be a factor. We already expect this given the constraints on the stability relations among the two feldspars with either muscovite or illite. Thus, it might be

that K-feldspar and chlorite are not both part of a local stable assemblage. Browne and Ellis (1970), Lonker et al. (1990), Browne and Simmons (2000), and Yang et al. (2001) provide detailed studies of the alteration mineralogy in the Ohaaki system. Browne and Ellis (1970) note that in the deep hot zones, there is some evidence that secondary chlorite forms later than secondary K-feldspar. There appears to be little evidence that secondary chlorite and K-feldspar form together at the same place and time.

The estimated deep water composition for various reactant mineral assemblages does not show much variation, despite the extensive reaction that occurs in the calculations. Table 1 shows the water composition based on (a) reaction with gas only, (b) reaction with gas, quartz, pyrite, albite, and K-feldspar and (c) reaction with gas, quartz, pyrite, albite, K-feldspar and ripidolite. Some components such as Li^+ and Rb^+ are invariant, as the modeling does not include them in the minerals considered. In reality, they would be affected particularly by the formation of many clay minerals. The Al^{3+} and Fe^{2+} concentrations for the gas only case are arbitrary small values. No matter what the mineral assemblage, the solution remains close to the equivalent of 0.05 m NaCl with 0.6 m dissolved CO_2 .

This initial modeling will serve as the foundation of additional modeling extending to the cooler parts of the system, laboratory experimentation, and a field test. The natural CO_2 levels deep in the Ohaaki geothermal system provide an excellent natural analog for rock-water-gas interactions in an EGS- CO_2 system having similar (felsic) rock type. Modeling, experimentation, and field testing will allow us to extend the upper limit of CO_2 concentration studied, although the natural values in this system are already

Table 1. Ohaaki deep water composition based on BR15 and reaction with gas and minerals for three cases. Concentrations are given in molality, oxygen fugacity in bars.

	Gas only, no minerals	Gas + quartz + pyrite + albite + K-feldspar	Gas + quartz + pyrite + albite + K-feldspar + ripidolite
Na ⁺	4.63 x 10 ⁻²	4.82 x 10 ⁻²	5.13 x 10 ⁻²
K ⁺	5.32 x 10 ⁻³	4.57 x 10 ⁻³	3.22 x 10 ⁻³
Li ⁺	1.66 x 10 ⁻³	1.66 x 10 ⁻³	1.66 x 10 ⁻³
Rb ⁺	2.11 x 10 ⁻⁵	2.11 x 10 ⁻⁵	2.11 x 10 ⁻⁵
Cs ⁺	1.17 x 10 ⁻⁵	1.17 x 10 ⁻⁵	1.17 x 10 ⁻⁵
Ca ²⁺	3.82 x 10 ⁻⁵	3.32 x 10 ⁻⁵	2.70 x 10 ⁻¹¹
Mg ²⁺	1.80 x 10 ⁻⁷	4.88 x 10 ⁻⁹	1.00 x 10 ⁻⁷
SiO _{2(aq)}	1.04 x 10 ⁻²	1.04 x 10 ⁻²	1.04 x 10 ⁻²
B(OH) _{3(aq)}	3.49 x 10 ⁻³	3.49 x 10 ⁻³	3.49 x 10 ⁻³
NH _{3(aq)}	1.18 x 10 ⁻⁴	1.18 x 10 ⁻⁴	1.18 x 10 ⁻⁴
CO _{2(aq)}	0.598	0.597	0.595
H _{2S} (aq)	3.94 x 10 ⁻³	3.88 x 10 ⁻³	3.05 x 10 ⁻³
Cl ⁻	4.53 x 10 ⁻²	4.53 x 10 ⁻²	4.53 x 10 ⁻²
SO ₄ ²⁻	7.78 x 10 ⁻⁵	8.91 x 10 ⁻⁵	1.86 x 10 ⁻⁶
HCO ₃ ⁻	7.41 x 10 ⁻³	8.44 x 10 ⁻³	1.03 x 10 ⁻²
HS ⁻	4.45 x 10 ⁻⁴	5.00 x 10 ⁻⁴	4.81 x 10 ⁻⁴
Al ³⁺	3.72 x 10 ⁻⁸	1.26 x 10 ⁻⁵	1.19 x 10 ⁻⁵
Fe ²⁺	1.54 x 10 ⁻¹⁰	2.14 x 10 ⁻⁸	8.76 x 10 ⁻⁸
pH	6.41	6.46	6.55
O ₂ fugacity	1.20 x 10 ⁻³²	1.07 x 10 ⁻³²	1.54 x 10 ⁻³³

relatively high. In future work we plan to elucidate in greater detail the thermodynamics and kinetics that pertain to both the Ohaaki geothermal system and an EGS-CO₂ system. Some of the questions to be answered are: Can K-feldspar and chlorite form simultaneously, or is the presence of one antithetical to the other? What is the role of kinetics and disequilibrium in controlling the relevant water-rock-gas interactions? Are some of the clay minerals produced in our calculations presented above really as stable as indicated? Are celadonites reasonable alteration products at Ohaaki, or are they reasonable proxies for the “illites” found there?

Conclusions

We have reviewed the status of knowledge of the Broadlands-Ohaaki geothermal system and concluded that it will serve as an excellent natural analog for rock-water-gas interactions in an EGS-CO₂ system. The range of rock types present in this system represent the more felsic side of silicate rocks, with the major rock types including greywacke, rhyolites, dacite, and equivalent pyroclastics. We have begun new geochemical modeling studies using a newer thermodynamic database and compared results with previous modeling studies. The principal secondary mineral assemblage described for the deep hot zone is not a stable mineral assemblage, and this raises questions about the stabilities of various

Wolery, Carroll

sheet silicate minerals in the natural system and in an EGS-CO₂ system. We will address these questions in additional modeling calculations, laboratory experiments, and a field study.

Acknowledgements

We thank Contact Energy Ltd. for assistance. We also thank Ed Mroczek and GNS Science, which is our research partner. This paper was improved by helpful comments from Andrew Rae of GNS Science and C.W. Klein of GeothermEx. This work was supported by the Geothermal Technologies Program of the U.S. Department of Energy. This work was performed under the auspices of the U.S. Department of Energy by Lawrence Livermore National Laboratory under Contract DE-AC52-07NA27344.

References

Brown, D.W., 2000. "A Hot Dry Rock Geothermal Energy Concept Using Supercritical CO₂ Instead of Water." *Proceedings of the Twenty-Fifth Workshop on Geothermal Reservoir Engineering*, Stanford University, pp. 233-238.

Browne, P.R.L., 1978. "Hydrothermal alteration in active geothermal fields." *Annual Reviews in Earth and Planetary Sciences*, v. 6, p. 229-250.

Browne, P.R.L., and A.J. Ellis, 1970. "The Ohaaki-Broadlands hydrothermal area, New Zealand: Mineralogy and related geochemistry." *American Journal of Science*, v. 269, p. 97-131.

Christenson, B.W., E.K. Mroczek, B.M. Kennedy, M.C. van Soest, M.K. Stewart, and G. Lyon, 2002. "Ohaaki reservoir chemistry: characteristics of an arc-type

hydrothermal system in the Taupo Volcanic Zone, New Zealand." *Journal of Volcanology and Geothermal Research*, v. 115, p. 53-82.

Giggenbach, W.F., 1989. "The chemical and isotopic position of the Ohaaki field within the Taupo Volcanic Zone." *Proceedings of the 11th New Zealand Geothermal Workshop*, p. 81-88.

Hedenquist, J.W., 1990. "The thermal and geochemical structure of the Broadlands-Ohaaki geothermal system, New Zealand." *Geothermics*, v. 19, p. 151-185.

Hemley, J.J., and W.R. Jones, 1964. "Aspects of the chemistry of hydrothermal alteration with emphasis on hydrogen metasomatism." *Economic Geology*, v. 59, p. 538-569.

Johnson, J.W., E.H. Oelkers, and H.C. Helgeson, 1992. "SUPCRT92: A software package for calculating the standard molal thermodynamic properties of minerals, gases, aqueous species, and reactions from 1 to 5000 Bar and 0 to 1000°C." *Computers & Geosciences*, v. 18, p.899-947.

Lee, S., and L. Bacon, 2000. "Operational history of the Ohaaki geothermal field, New Zealand." *Proceedings of the World Geothermal Congress, Kyushu-Tohoku, Japan, May 28-June 10, 2000*.

Lonker, S.W., J.D. Fitz Gerald, J.W. Hedenquist, and J.L. Walshe, 1990. "Mineral-fluid interactions in the Broadlands-Ohaaki Geothermal System, New Zealand." *American Journal of Science*, v. 290, p. 995-1068.

McGrail, B.P., H.T. Schaef, V.-A. Glezakou, L.X. Dan, and A.T. Owen, 2009. "Water reactivity in the liquid and

Wolery, Carroll

supercritical CO₂ phase: Has half the story been neglected?" *Energy Procedia*, v. 1, p. 3415-3419.

Pruess, K., 2006. "Enhanced Geothermal Systems (EGS) Using CO₂ as Working Fluid – a Novel Approach for Generating Renewable Energy with Simultaneous Sequestration of Carbon." *Geothermics* v. 35, pp. 351-367.

Reed, M.H., 1982. "Calculation of multicomponent chemical equilibria and reaction processes in systems involving minerals, gases, and an aqueous phase." *Geochimica et Cosmochimica Acta*, v. 46, p. 513-528.

Reed, M.H. and N.F. Spycher, 1985. "Boiling, cooling, and oxidation in epithermal systems: A numerical modeling approach." *Reviews in Economic Geology*, v. 2, p. 249-272.

Regnault, O., V. Lagneau, H. Catalette, and H. Schneider, 2005. "Étude expérimentale de la réactivité du CO₂ supercritique vis-à-vis de phase minerals pure. Implications pour la séquestration géologique de CO₂." *C.R. Geoscience*, v. 337, p. 1331-1339.

Rimstidt, J.D., 1997. "Quartz solubility at low temperatures." *Geochimica et Cosmochimica Acta*, v. 61, p. 2553-2558.

Simmons, S.F., and P.R.L. Browne, 2000. "Hydrothermal minerals and precious metals in the Broadlands-Ohaaki geothermal system: Implications for understanding low-sulfidation epithermal environments." *Economic Geology*, v. 95, p. 971-999.

Span, R., and W. Wagner, 1996. "A new equation of state for carbon dioxide covering the fluid region from the triple-point temperature to 1100K at pressures up to

800MPa." *Journal of Physical and Chemical Reference Data*, v. 25, p. 1509-1596.

Wolery, T.J., 1978. "Some Chemical Aspects of Hydrothermal Processes at Mid-Oceanic Ridges - A Theoretical Study. I. Basalt-Sea Water Reaction and Chemical Cycling Between the Oceanic Crust and the Oceans. II. Calculation of Chemical Equilibrium Between Aqueous Solutions and Minerals." Ph.D. dissertation. Evanston, Illinois: Northwestern University.

Wolery, T.J., and R.L. Jarek, 2003. "Software User's Manual, EQ3/6 version 8.0." OCRWM M&O Contractor, Las Vegas, Nevada.

Wolery, T.J., and C.F. Jove-Colon, Originators. 2007. "Qualification of Thermodynamic Data for Geochemical Modeling of Mineral-Water Interactions in Dilute Systems." ANL-WIS-GS-000003 Rev 01, Sandia National Laboratories, Las Vegas, Nevada.

Xu, T., K. Pruess, and J. Apps, 2008. "Numerical Studies of Fluid-Rock Interactions in Enhanced Geothermal Systems (EGS) with CO₂ as Working Fluid." *Proceedings of the Thirty-Third Workshop on Geothermal Reservoir Engineering*, Stanford University.

Yang, K., P.R.L. Browne, J.F. Huntington, and J.L. Walshe, 2001. "Characterising the hydrothermal alteration of the Broadlands-Ohaaki geothermal system, New Zealand, using short-wave infrared spectroscopy." *Journal of Volcanology and Geothermal Research*, v. 106, p. 53-65.